INTRAFRACTIONAL PROSTATE MOTION MANAGEMENT WITH THE CLARITY AUTOSCAN SYSTEM

Martin Lachaine and Tony Falco

Elekta Ltd., Montréal, Québec, Canada

Abstract— Intrafractional motion of the prostate can be significant, and its management is of particular importance for hypofractionated regimes and stereotactic ablative radiotherapy (SABR). In this paper, we describe the Clarity Autoscan with Monitoring system and its use of non-invasive soft tissue imaging to monitor prostate motion during the course of radiotherapy. The system uses a 4D autoscan ultrasound probe to image the prostate through the acoustic window of the perineum. We discuss this imaging technique, as well as the algorithms used to track the prostate during treatment. We measure the accuracy of the tracking algorithm with a motion phantom and find it to be -0.2 ± 0.2 mm, 0.2 ± 0.4 mm and -0.0 ± 0.2 mm in the A/P, L/R and S/I directions, respectively.

Keywords— radiotherapy, prostate, motion management, intrafractional motion, ultrasound.

INTRODUCTION

Interfractional image guidance for external beam radiotherapy of the prostate has emerged as an integral part of conformal and intensity modulated radiation therapy (IMRT) treatments. The prostate position can vary substantially between the initial simulation and each day of treatment, and thus can benefit dosimetrically from pre-treatment corrections [1]. Fiducial-based planar x-ray methods (kilovoltage [2] or megavoltage [3]), tomographic CT (cone-beam [4] or conventional [5]), transabdominal ultrasound (TAUS) [6,7] and electromagnetic beacons have been used for this purpose [8].

The magnitude of intrafractional corrections is on average smaller than interfractional motion. Large excursions greater than 1 cm may occur in some fractions, although the dosimetric advantage of corrections is diminished when averaged over a conventional fractionation regime [9,10]. Although it can be argued that it is important to ensure that dose is correctly delivered to the target even under conventional fractionation, the real advantage to intrafractional motion corrections emerges for hypofractionated regimes and stereotactic ablative radiotherapy (SABR) treatments.

Various technologies have been reported for prostate motion management. Stereoscopic x-ray imaging with kilovoltage (kV) x-rays acquires two planar projections using digital x-ray detectors placed in orthogonal directions around the patient. Since planar x-ray imaging cannot visualize soft tissue, fiducials are implanted within the prostate with needles inserted transperineally under transrectal ultrasound guidance. Stereoscopic kV imaging is commonly used for interfractional patient positioning. For intrafractional correction, however, the extra imaging dose limits the sampling rate, for example one image per 30 seconds [11].

Some research articles have explored using the megavoltage (MV) energy treatment beam to track fiducials in the prostate. The images are acquired with an electronic portal imaging device (EPID). The advantage of this technique is that no additional imaging dose is delivered, since the treatment beam is already being used for treatment delivery.

One limitation of the MV tracking technique is that motion of the prostate is only known in the direction perpendicular to the beam at any moment in time (the direction of the beam changes throughout treatment, either step-wise or continuously). To circumvent this, assumptions are made about the prostate motion – *e.g.*, that it is confined to the sagittal plane, and that motion in the anterio-posterior direction is proportional to motion in the superior-inferior direction. For this reason, this technique is approximate only and is considered as a *failure detection strategy – i.e.*, an indication that there is a high probability that the prostate has moved outside of tolerance. Detection of failure would then warrant a more precise localization measurement to effectuate a correction with, for example, cone-beam CT or stereoscopic imaging [12,13].

Another limitation of MV imaging to measure intrafractional motion is that for IMRT treatments, the aperture of the treatment beam may not encompass all or any fiducials at any given point in time. There is thus a certain fraction of dose delivery where the tracking is lost. This technique has not to our knowledge been implemented commercially to date.

Another technique to monitor intrafractional motion is the use of transponders (beacons) which are implanted in the prostate, their positions tracked in time using an array of alternating current magnetic coils to generate a resonant response. This concept is used by the Calypso

System (Varian Medical Systems, Palo Alto, CA) [8]. In this solution, the detecting array is placed above the patient and is tracked with three optical cameras calibrated to the room isocenter.

In the Calypso beacon technique, individual beacons 8 mm × 2 mm in size are inserted into the prostate via needles through the perineum under transrectal ultrasound guidance. A minimum of 2 beacons, preferably 3 or more, are used for a given patient. Comparison of the beacon centroid to its position in the planning CT is used to first align the patient for interfractional motion. During treatment delivery, the centroid of the implanted beacons are monitored at high temporal frequency. This technique has been used successfully for intrafractional motion of the prostate. Some limitations include the invasiveness of the procedure, as beacons are generally larger than conventional fiducials used with x-ray imaging; beacon cost; lack of soft tissue information; and MRI artifacts [14] in post-treatment follow-up.

As motion management of the prostate gains importance, particularly for SABR and hypofractionated regimes, intrafractional monitoring of soft-tissue without the need for implanted fiducials or additional radiation dose could have significant benefits. One potential technique would be an integrated MRI-linac, which would give excellent soft tissue definition throughout the treatment. This technology is being developed [15] and has promise to become the gold standard for motion management.

Ultrasound is another non-invasive and non-ionizing imaging technology which has potential benefits such as lower cost than MRI, while retaining excellent soft tissue definition of the prostate. This paper investigates the use of ultrasound for prostate motion management, with a focus on describing the implementation and use of the *Clarity Autoscan with Monitoring* system which has been designed for this purpose.

ULTRASOUND SYSTEMS FOR IMAGE GUIDANCE

Ultrasound has been commonly used for pre-treatment interfractional corrections. The BAT system (Best Medical, Springfield, Virginia) uses transabdominal ultrasound (TAUS) to image the prostate in two near-orthogonal slices through the prostate; the orientation of the slices are known with respect to the treatment room [6]. The prostate contour from the treatment plan is visually matched to the prostate as seen on the ultrasound images, and the resulting prostate shift is corrected with a translation of the treatment couch.

The Sonarray System (Varian Medical Systems, Palo Alto, CA) acquires a freehand sweep of the ultrasound probe to generate a multitude of slices through the prostate, while simultaneously tracking the position and orientation of each slice with respect to the isocenter room coordinates [16]. The slices are reconstructed into a 3D voxel image in room coordinates to be used for alignment purposes. As with the BAT system, the prostate contour from the CT treatment plan is matched to the ultrasound image to measure and correct for prostate displacement.

AAPM Task Group 154, *Quality Assurance for ultrasound-guided radiotherapy*, recommends that ultrasound image guidance use an ultrasound image as reference rather than a CT treatment planning contour [17]. This allows comparison of the same modality from simulation to treatment, eliminating the judgment required to align ultrasound and CT images.

The Clarity System (Elekta, Stockholm, Sweden) uses TAUS imaging of the prostate to acquire a freehand sweep in both the CT-sim and treatment rooms. The Clarity tracking system detects an array of infrared reflectors affixed to the probe handle throughout the sweep. The sweeps are reconstructed to generate 3D ultrasound images in each room. Ultrasound images acquired prior to each treatment are compared to reference ultrasound images from CT-Sim to calculate and correct for interfractional prostate motion. This intramodality comparison has been shown to be more accurate than the intermodality method of comparing ultrasound to CT [7]. The Clarity System has also been extended to other treatment sites such as breast [18,19]. In the remainder of this article, we will describe the extension of the Clarity System to monitoring intrafractional motion; this system will be referred to as *Clarity Autoscan with Monitoring*.

The ultrasound-based systems described above rely on TAUS techniques for external beam radiotherapy image guidance. TAUS uses the acoustic window of the bladder to obtain prostate images. Limitations include the necessity of bladder filling as well as shadowing of the prostatic apex in some patients by the pubic symphisis. TAUS is not well-suited to intrafractional motion monitoring, as the probe lies in the radiation path of typical prostate treatment beam arrangements.

ALTERNATIVE ULTRASOUND TECHNIQUES

Transrectal ultrasound (TRUS) is seen as the gold standard of ultrasound techniques for measuring prostate volumes. TRUS, however, is not practical for external beam radiotherapy due to the proximity of the probe to the prostate, deformation of the prostate by the probe, as well as patient acceptability during multiple fractions.

Transperineal ultrasound (TPUS) is not a well- known technique for prostate imaging and is primarily used for patients that cannot tolerate TRUS. It is an interesting

candidate for intrafractional motion detection, however, since the probe lies between the patient's legs and is thus outside of the radiation path. It also has the potential for high image quality due to the short path between the perineum and the prostate.

Rathaus *et al* [20] have studied TPUS imaging in 80 patients with benign prostatic hyperplasia, and compared the measured prostatic volume with the actual weight of the surgically removed gland and found good correlation between the two (0.89). They used an approximate ellipsoidal formula to calculate volume since they did not have 3D images, which can reduce the accuracy of their prostate volume calculations. They experienced technical difficulties in approximately 10% of patients which had prominent pubic bones, due to the acoustic shadows from these bones. This should not present any issues for motion management for this subset of patients as long as there is sufficient prostate in the image to track motion.

Griffiths *et al* [21] have compared TRUS with TPUS in 287 healthy men. They used the ellipsoidal approximation for prostate volume since they did not have 3D ultrasound. When considering TRUS as the gold standard, they found excellent volume agreement with minimal downward bias (-3.7%) for total prostate volume. They had a technical failure rate of 13.6% for TPUS, similar to that experienced by Rauthaus *et al*.

In a study of 50 patients, Terris *et al* [22] were able to obtain good TPUS visualization of the prostate in 96% (transverse plane) and 90% (sagittal plane). Using a 2D spheroid approximation for volume, they found that prostate volumes correlated well between TRUS and TPUS (r = 0.876). They found that TPUS was able to identify some intraprostatic findings (*e.g.*, calcification and cysts), but not suspicious hypoechoic lesions. They expect that large prostatic tumors could be detected with TPUS, but that it may not be able to detect smaller tumors. Any visualization of tumors would be an added benefit to treatment planning but not a requirement for monitoring the prostate position.

AUTOSCAN IMAGE ACQUISITION

The Clarity System for interfractional image guidance uses a reconstructed sweep from a tracked 2D ultrasound probe to form 3D images. Although this is adequate for pre-treatment corrections, it is not practical for intrafractional motion management as the therapist is not present in the treatment room during radiation beam delivery. An automatically scanning probe, or *autoscan probe*, is therefore a necessity for this application.

The *Clarity Autoscan* system has integrated a mechanically-scanned autoscan probe for this purpose. The probe consists of a 2D probe within housing, with motorized control of the sweeping motion. The probe is able to scan a complete 75º sweep in 0.5 seconds. The patient does not sense any motion other than a slight vibration, as all motion is internal to the probe housing.

The autoscan probe has an integrated homing sensor which triggers as it passes through the center. This allows every sweep to be checked for geometrical accuracy, which is critically important for this application.

The autoscan probe is housed within an *Autoscan Probe Kit* (ASPK), shown in Fig 1. The ASPK consists of a base plate, which can be indexed to the CT and treatment room couches. The Autoscan probe is attached to the base and allows positioning and locking of the probe for TPUS scanning, as well as incorporating a fine adjust mechanism. An array of 4 infrared reflective makers are affixed to the probe so that its position and orientation can be detected by the Tracking System.

CALIBRATION

Figure 1Autoscan Probe Kit for transperineal ultrasound of the prostate

The Clarity Autoscan System must be calibrated to the coordinate system of the CT and treatment room, respectively. This provides a relationship between each ultrasound pixel and their corresponding position in room coordinates. We may define the following four coordinate systems: **R** is the room coordinate system, **T** is the coordinate system of the tracker, **F** is the coordinate system of a given 2D ultrasound frame, and **P** is the probe coordinate system defined by the definition of the reflective marker array attached to its handle. As illustrated in Fig. 2, a pixel in ultrasound "frame" coordinates $\boldsymbol{r}_{\mathrm{F}}$ can be transformed to room coordinates $\boldsymbol{r}_R$ by the equation

$$\boldsymbol{r}_R = {}^{R}\boldsymbol{T}_{T}\,{}^{T}\boldsymbol{T}_{P}\,{}^{P}\boldsymbol{T}_{F}\boldsymbol{r}_{F} \qquad (1)$$

where ${}^{P}\boldsymbol{T}_{F}$ is the 4×4 frame-to-probe transformation matrix, ${}^{T}\boldsymbol{T}_{P}$ is the probe-to-tracker transformation matrix, and ${}^{R}\boldsymbol{T}_{T}$ is the tracker-to-room transformation matrix. *Room calibration* and *probe calibration* are defined as finding the transformations ${}^{R}\boldsymbol{T}_{T}$ and ${}^{P}\boldsymbol{T}_{F}$, respectively. The former is static as long as the isocenter and tracking system do not change, and the latter as long as the markers affixed to the probe's handle maintain a constant relationship.

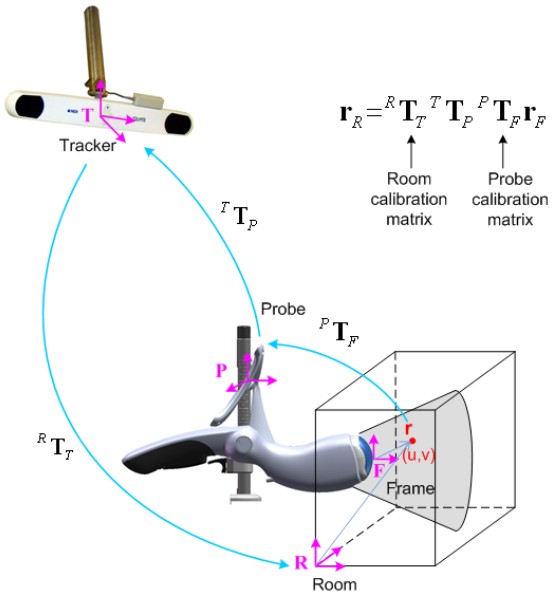

Figure 2. Schematic diagram illustrating coordinate transformations for calibration

The frame-to-probe matrix can be further broken down into the components

$$ {}^{P}\boldsymbol{Tr}_{F} = {}^{P}\boldsymbol{T}_{C}\boldsymbol{T}_{S}\,{}^{C}\boldsymbol{Tr}_{F}(i) \qquad (2) $$

where the frame-to-center rotation matrix ${}^{C}\boldsymbol{T}_{F}(i)$ defines the rotation of the frame relative to the probe as a function of indexed motor position i, $\boldsymbol{T}_{S}$ is a scaling matrix and ${}^{P}\boldsymbol{T}_{C}$ is the center-to-probe transformation, which defines the relationship between the central frame when the probe is at its center position and the marker array affixed to the probe handle.

Room Calibration is defined by aligning etchings on the Clarity calibration phantom (Fig. 3) to the isocentric room lasers, and pressing a *Calibrate* button on-screen. The tracking system then detects infrared markers affixed to the front plate of the phantom, and and since the relationship between these markers and the etchings on the phantom is known, the room calibration matrix can be calculated.

The probe calibration procedure is performed by acquiring a 3D image of the calibration phantom with the autoscan probe. The phantom contains rods and spheres at known positions; the positions are known *a priori* but are adjusted by measurements of the distances on a CT phantom. The rods and spheres are automatically detected in the ultrasound images, and an optimization algorithm is used to find the optimal ${}^{P}\boldsymbol{T}_{F}$ that best fits the detected positions to their known positions in the phantom. This is saved in the Clarity System as the probe calibration, which along with the room calibration is used to convert all ultrasound images (frames) along with their tracking system readings ${}^{T}\boldsymbol{T}_{P}$ into room coordinates using Equation (1).

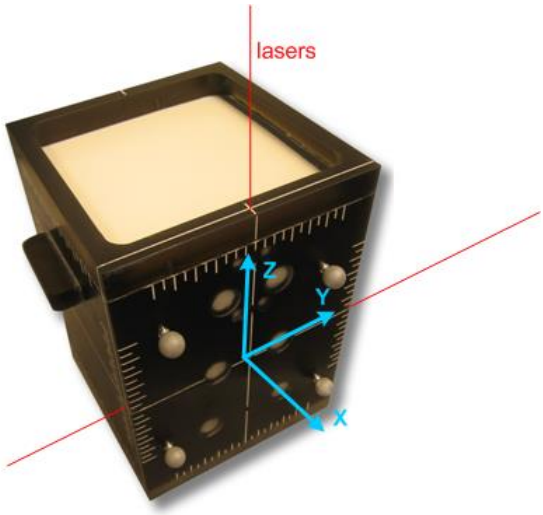

Figure 3 Clarity phantom used for calibration

Calibration is performed upon installation, and in theory would not change unless a) the probe were deformed, b) the camera moved relative to isocenter, or c) the isocentric coordinate system were moved. This is verified daily by a Quality Control (QC) procedure which consists of scanning a sphere in the Clarity phantom and comparing its detected location with its location as measured on CT. Calibration may be repeated in the event the QC is out of tolerance.

IMAGING ACCURACY AND PRECISION

In order to validate accuracy and precision of the calibrated Autoscan image acquisition process, we used the Clarity phantom which has embedded sphere and rod structures at known positions that can be visualized on both CT and ultrasound.

CT and Clarity Autoscan images of the phantom were successively acquired and registered as per clinical workflow. Since the systems are calibrated to each other, structures in the phantom should be aligned in the fused images. We validated this by reviewing the resulting fusions (Fig. 4) in the Clarity Workstation for three successive scans with different probe and phantom combinations. All structures were visually validated to be within 1 mm of each other on both modalities.

To quantify the precision, we scanned the same phantom 32 times, automatically segmented the phantom sphere in each scan, and calculated the resulting structure centroid for each scan. The 95% prediction interval for the centroid position were found to be ±0.4 mm, ±0.7 mm and ±0.5 mm, and the standard deviations 0.1 mm, 0.2 mm and 0.1 mm in the SUP/INF, RT/LT and ANT/POST directions, respectively. A histogram of the results is shown in Fig. 5.

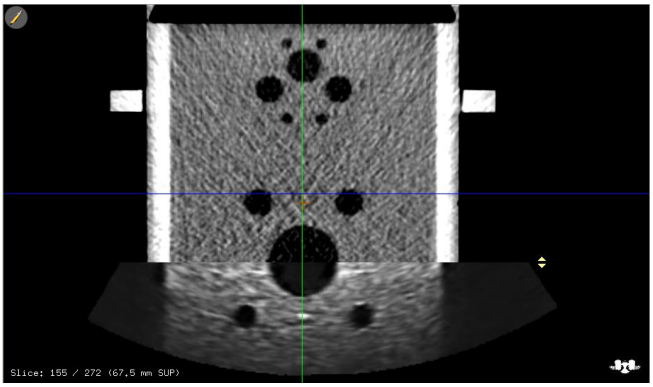

Figure 4. Registered CT and Clarity Autoscan images on the same phantom for validation of registration

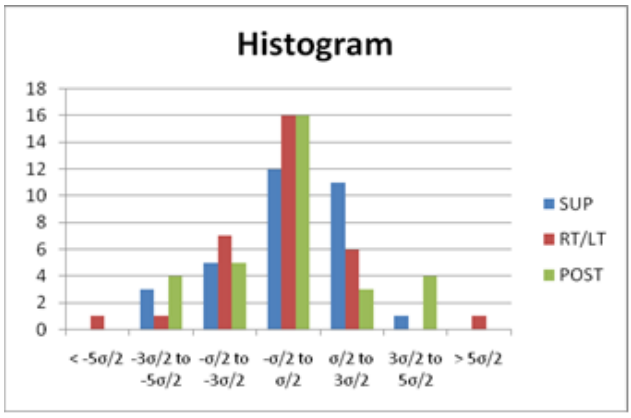

Figure 5. Histogram of precision measurements

INTRAFRACTION PROSTATE MONITORING

In order to monitor the prostate during treatment, the autoscan probe must continually sweep through a sector which includes the prostate. The ultrasound frame-rate is on the order of 45 Hz, depending on the imaging parameters used. The relationship between the angular spacing between frames $\Delta\theta$, the total sweep time T_{sweep}, the maximum sweep angle $\Delta\theta_{sweep}$ and the ultrasound frame rate F is given by

$$T_{sweep}\Delta\theta = \frac{\Delta\theta_{sweep}}{F} \quad . \qquad (3)$$

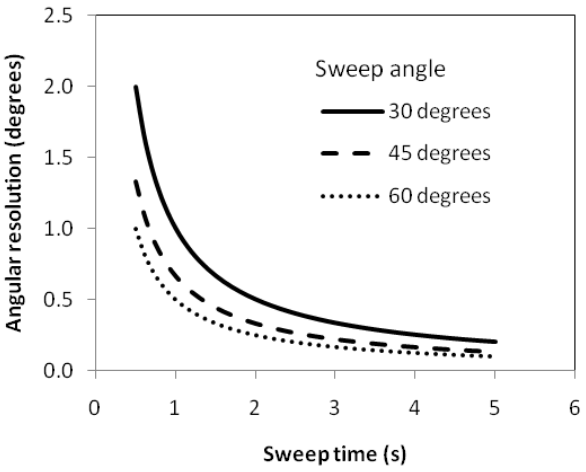

Figure 6. Theoretical plot showing relationship between angular resolution and sweep time for different sweep angles, assuming an ultrasound frame rate of 45 Hz.

It can be seen that there is a trade-off between the sweep time and resolution as defined by the angular spacing. The relationship, assuming a frame rate of 45 Hz, is plotted in Fig. 6. From the graph, a 45º sweep with an angular resolution of 0.3º would lead to a 2.5 second sweep time.

Although the maximum sweep angle is possible with the autoscan probe, we have found that a 45 º is a good trade-off to obtain sufficient coverage of the prostate for TPUS imaging. Assuming a typical prostate depth of 5 cm, this would lead to a resolution of 0.9 mm at the middle at the depth of the prostate. From the graph, the sweep time for this scenario would be approximately 1 second.

Even if a high monitoring sampling is possible, clinical use of prostate motion management during external beam radiotherapy generally compensates for drifts and stable excursions rather than chase transient peaks. We have thus implemented a slower sweep time of 2.5 seconds to gain higher resolution soft tissue imaging - a 0.4º angular

resolution which would result in a 0.35 mm resolution at 5 cm depth.

In the Clarity Autoscan with Monitoring system, a full pre-treatment sweep is first acquired, and the images reconstructed and displayed to the user. This image is then compared to the simulation 3D ultrasound image to calculate a couch shift to correct for interfractional prostate motion. The system then goes into a *monitoring* phase, where the ultrasound sweeps back and forth continuously. The first sweep is used as a reference for monitoring. The image is continuously refreshed as the autoscan probe sweeps the region of interest.

An intensity-based image-to-image registration finds an optimal fit between the current image and the monitoring reference image. The algorithm uses normalized cross-correlation as the cost-function, and uses pixels within a 2 cm boundary surrounding the prostate for the comparison. The registration is constrained to 6 degrees of freedom, *i.e.*, translations and rotations with no deformations.

Image-to-image registrations are most commonly performed in rectilinear coordinate systems. For the current monitoring application, the ultrasound sweeps are acquired in a cylindrical coordinate system (Fig. 7). To reduce calculation time, we skip the step of reconstruction in the monitoring algorithm and directly register images in cylindrical coordinates [23]. The calculation time for each registration is approximately 0.7 seconds. Rather than wait for a full sweep, the calculation is applied in succession on each partially updated image.

The registration algorithm calculates a correlation score for each iteration. This score would be 1 for a perfectly correlated fit, and 0 for a completely uncorrelated fit. We have chosen a cut-off based on training data; the user is alerted to verify the registration on-screen if the correlation is below the threshold. This provides an additional safety measure.

During monitoring, the user is presented with sagittal and coronal views, as well as the current live image, as shown in Fig. 8. Each view shows a contour overlay of the prostate as calculated by the registration. Graphs showing the motion in each Cartesian direction are plotted, as when thresholds are exceeded. The system provides an alert when the threshold has been exceeded by a certain amount of time. The therapist would then interrupt the treatment, perform a couch correction, and resume treatment. Thresholds in each direction, as well as time-out-of-threshold values, are pre-determined by the physician prior to the first treatment fraction.

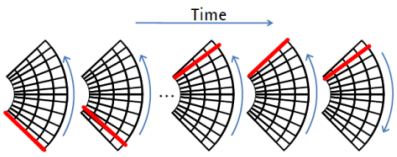

Figure 7. Cylindrical coordinate system geometry

PHANTOM MEASUREMENTS

In order to validate the prostate monitoring algorithm, a commercially available multimodality pelvic phantom (CIRS), modified with an extra acoustic window on one side to accommodate TPUS scanning geometry, was placed on a robotic translation stage (Velmex, Bloomfield, NY), as shown in Fig 9. The autoscan probe was set up to continuously acquire images of the phantom. A reflective marker array was affixed to the top of the phantom to record the actual motion of the phantom with the Clarity tracking system.

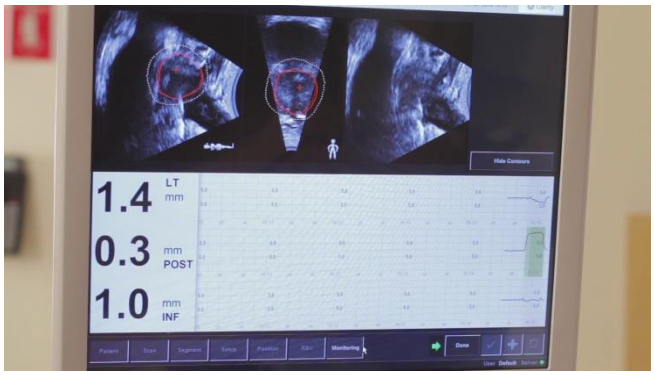

Figure 8. Clarity Monitoring screen

The robotic stage was programmed with motion patterns, and the prostate structure was tracked with Clarity to quantify the differences between the calculated and programmed time sequences. Motion in the A/P and L/R plane was measured differently than that in the S/I direction due to the practical issue of maintaining contact between the probe and the phantom as the phantom is moved. For the former, a rectangular wave was programmed with ±10 mm in the A/P direction and ±5 mm in the L/R direction. Each step was held for a duration of 10 minutes, and run 5 times in a row for a total of 10 minutes. For the S/I motion, a gel pad was used between the phantom and the probe to maintain contact, and the motion amplitude was limited to ±4 mm.

The results are shown in Fig. 10 for the A/P and L/R directions, and in Fig. 11 for the S/I direction. The mean and standard deviation of the differences are -0.2 ± 0.2 mm, 0.2 ± 0.4 mm and -0.0 ± 0.2 mm in the A/P, L/R and S/I directions, respectively. The calculated versus programmed motion was within 1 mm 95% of the time.

Abramowitz *et al* [24] also performed measurements with the Clarity Autoscan system at the University of Miami. They used a motorized phantom with an embedded prostate-like structure submerged in a liquid. While Clarity tracked the structure, the Calypso System (Varian Medical Systems, Palo Alto, CA) tracked beacons affixed to an external stem that followed the same motion as the prostate structure. They programmed 7 series of clinical prostate motion datasets from the literature, and found excellent agreement between Calypso and Clarity.

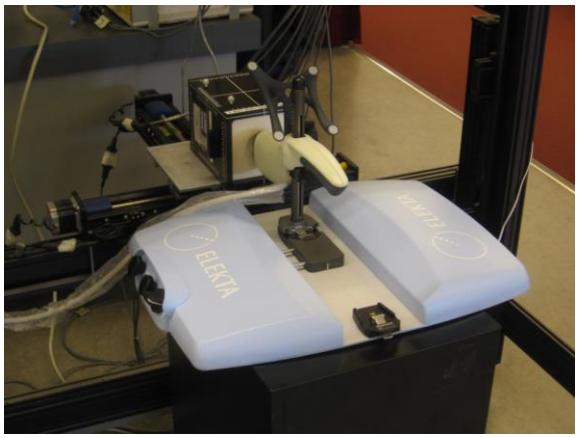

Figure 9.Experimental set-up for phantom measurements

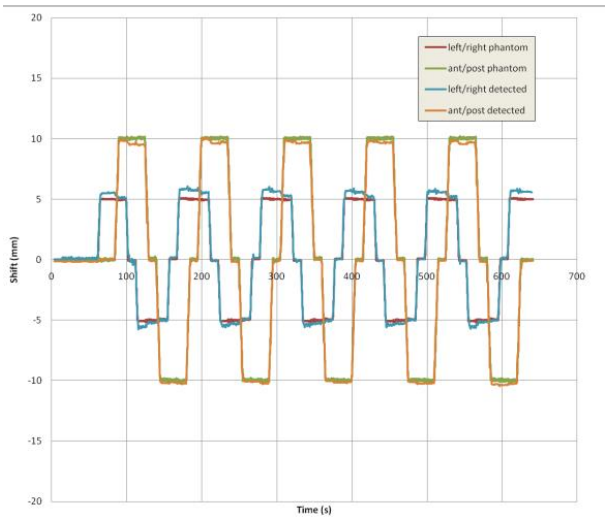

Figure 10. Comparison of programmed versus calculated motion in A/P and L/R directions

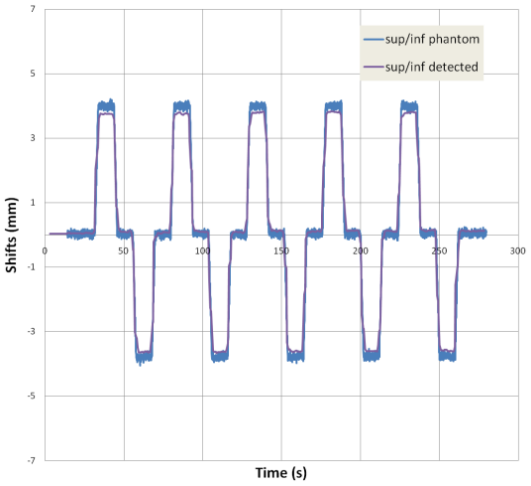

Figure 11. Comparison of programmed versus calculated motion in S/I directions

PATIENT IMAGING

Wallace *et al* [25] studied the use of Clarity Autoscan transperineal imaging on a series of 15 patients. They acquired autoscan TPUS as well as freehand TAUS images for each patient during the CT simulation process. Image quality of prostate borders for TPUS was similar for TAUS except for a dramatically improved visualization of the prostatic apex. Rectum and penile bulb visualization was much improved over TPUS, whereas the bladder was better visualized under TAUS. Example images acquired during the study are shown in Figs 12 and 13.

Abramowitz *et al* [26] collected data during external beam radiotherapy treatments for prostate cancer for 62 fractions. They found that the tracking algorithm accurately tracked observed intrafractional prostate motion throughout the series.

Further comparative clinical studies are ongoing and will be presented by the principal investigators in separate manuscripts.

CONCLUSION

We present a system for intrafractional prostate motion management during external beam radiotherapy. The system relies on soft tissue imaging of the prostate with transperineal ultrasound without the need for implanted fiducials or extra imaging dose. A calibration algorithm has been described which brings the imaging data in the isocentric treatment coordinates, and a registration algorithm is described which successfully tracks the prostate during treatment. Accuracy and precision of imaging, as well as the prostate monitoring algorithm, are found to be less than 1 mm in each direction. Future work will investigate intrafractional monitoring of surrounding critical structures, as well as extension to other anatomical treatment sites.

ACKNOWLEDGMENT

The authors would like to acknowledge Rupert Brooks and Fabienne Lathuilière for internal reports referred to in this paper as well as useful discussions.

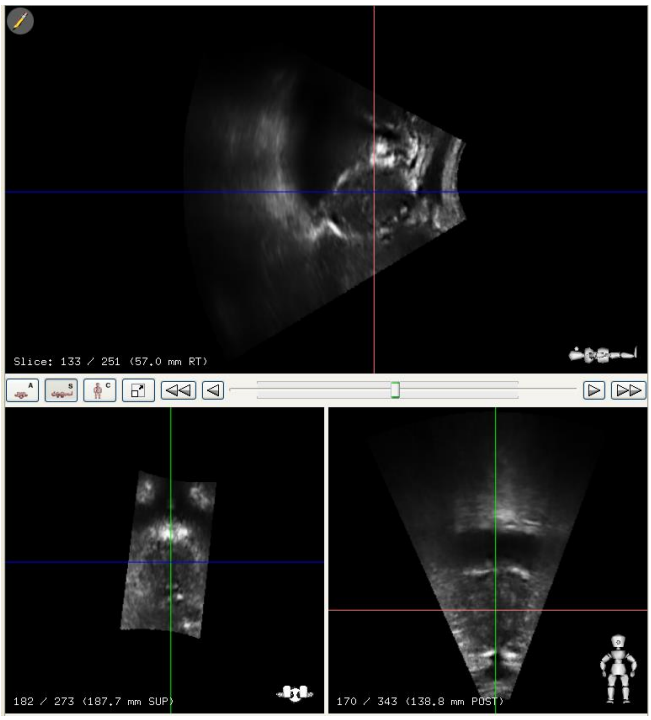

Figure 12. Clarity Autoscan image of the prostate for a sample patient

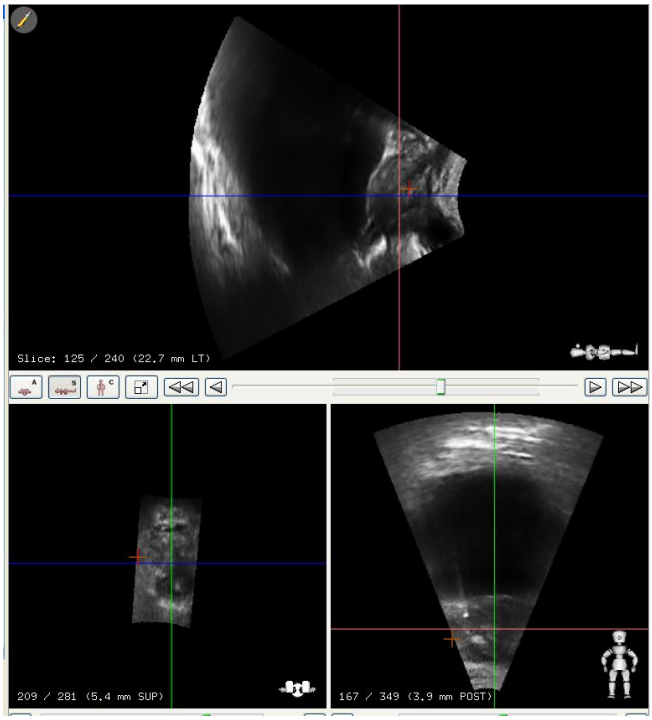

Figure 13. Clarity Autoscan image of the prostate for a sample patient

REFERENCES

1. Thongphiew D, Wu QJ, Lee WR, et al. Comparison of online igrt techniques for prostate imrt treatment: Adaptive vs repositioning correction. Med. Phys. 2009;36:1651-1662.
2. Gauthier I, Carrier JF, Beliveau-Nadeau D, et al. Dosimetric impact and theoretical clinical benefits of fiducial markers for dose escalated prostate cancer radiation treatment. Int. J. Radiat. Oncol. Biol. Phys 2009;74:1128-1133.
3. Vetterli D, Thalmann S, Behrensmeier F, et al. Daily organ tracking in intensity-modulated radiotherapy of prostate cancer using an electronic portal imaging device with a dose saving acquisition mode. Radioth. Oncol. 2006;79:101-108.
4. Jaffray DA, Siewerdsen JH, Wong JW, et al. Flat-panel cone-beam computed tomography for image-guided radiation therapy. Int. J. Radiat. Oncol. Biol. Phys 2002;53:1337-1349.
5. Owen R, Kron T, Foroudi F, et al. Comparison of ct on rails with electronic portal imaging for positioning of prostate cancer patients with implanted fiducial markers. Int. J. Radiat. Oncol. Biol. Phys 2009;74:906-912.
6. Lattanzi J, McNeeley S, Donnelly S, et al. Ultrasound-based stereotactic guidance in prostate cancer--quantification of organ motion and set-up errors in external beam radiation therapy. Comp. Surg. 2000;5:289-295.
7. Cury FL, Shenouda G, Souhami L, et al. Ultrasound-based image guided radiotherapy for prostate cancer: Comparison of cross-modality and intramodality methods for daily localization during external beam radiotherapy. Int. J. Radiat. Oncol. Biol. Phys 2006;66:1562-1567.
8. Kupelian P, Willoughby T, Mahadevan A, et al. Multi-institutional clinical experience with the calypso system in localization and continuous, real-time monitoring of the prostate gland during external radiotherapy. Int. J. Radiat. Oncol. Biol. Phys 2007;67:1088-1098.

9. Langen KM, Willoughby TR, Meeks SL, et al. Observations on real-time prostate gland motion using electromagnetic tracking. Int. J. Radiat. Oncol. Biol. Phys 2008;71:1084-1090.
10. Li HS, Chetty IJ, Enke CA, et al. Dosimetric consequences of intrafraction prostate motion. Int. J. Radiat. Oncol. Biol. Phys 2008;71:801-812.
11. Xie Y, Djajaputra D, King CR, et al. Intrafractional motion of the prostate during hypofractionated radiotherapy. Int. J. Radiat. Oncol. Biol. Phys 2008;72:236-246.
12. Liu W, Luxton G Xing L. A failure detection strategy for intrafraction prostate motion monitoring with on-board imagers for fixed-gantry imrt. Int. J. Radiat. Oncol. Biol. Phys 2010;78:904-911.
13. Liu W, Qian J, Hancock SL, et al. Clinical development of a failure detection-based online repositioning strategy for prostate imrt--experiments, simulation, and dosimetry study. Med. Phys. 2010;37:5287-5297.
14. Zhu X, Bourland JD, Yuan Y, et al. Tradeoffs of integrating real-time tracking into igrt for prostate cancer treatment. Phys. Med. Biol. 2009;54:N393-401.
15. Lagendijk JJ, Raaymakers BW, Raaijmakers AJ, et al. Mri/linac integration. Radioth. Onc. 2008;86:25-29.
16. Tome WA, Meeks SL, Orton NP, et al. Commissioning and quality assurance of an optically guided three-dimensional ultrasound target localization system for radiotherapy. Med. Phys. 2002;29:1781-1788.
17. Molloy JA, Chan G, Markovic A, et al. Quality assurance of u.S.-guided external beam radiotherapy for prostate cancer: Report of aapm task group 154. Med. Phys. 2011;38:857-871.
18. Berrang TS, Truong PT, Popescu C, et al. 3d ultrasound can contribute to planning ct to define the target for partial breast radiotherapy. Int. J. Radiat. Oncol. Biol. Phys 2009;73:375-383.
19. Wong P, Muanza T, Reynard E, et al. Use of three-dimensional ultrasound in the detection of breast tumor bed displacement during radiotherapy. Int. J. Radiat. Oncol. Biol. Phys 2011;79:39-45.
20. Rathaus V, Richter S, Nissenkorn I, et al. Transperineal ultrasound examination in the evaluation of prostatic size. Clinical radiology 1991;44:383-385.
21. Griffiths KA, Ly LP, Jin B, et al. Transperineal ultrasound for measurement of prostate volume: Validation against transrectal ultrasound. J. Urology 2007;178:1375-1379.
22. Terris MK, Hammerer PG Nickas ME. Comparison of ultrasound imaging in patients undergoing transperineal and transrectal prostate ultrasound. Urology 1998;52:1070-1072.
23. Brooks R. Intrafraction prostate motion correction using a non-rectilinear image frame. In Madabhushi, A. et. al (Eds.): Proceedings of the International Workshop on Prostate Cancer Imaging. Image Analysis and Image-Guided Interventions, in conjunction with MICCAI 2011. Toronto, Canada, Sept 22, 2011.
24. Abramowitz M, E. B, R. F, et al. Noninvasive real-time prostate tracking using a transperineal ultrasound approach Int. J. Radiat. Oncol. Biol. Phys 2012;84:S1338.
25. Wallace HJ, Hard D, Archambault J, et al. Autoscan transperineal ultrasound of the pelvis for prostate gland localization - a feasibility study. Int. J. Radiat. Oncol. Biol. Phys;84:S373.
26. Abramowitz MC, Freedman L, Iskanian A, et al. Noninvasive real-time prostate tracking using a transperineal ultrasound approach. Proceedings of the 95th American Radium Society (in press).
27.

Corresponding author:

Author:	Martin Lachaine
Institute:	Elekta Ltd
Street:	2050 rue Bleury, Suite 200
City:	Montréal, Québec
Country:	Canada
Email:	martin.lachaine@elekta.com